

Protein tyrosine phosphatase PRL-3 in malignant cells and endothelial cells: expression and function

Cecile Rouleau, Andre Roy, Thia St. Martin, Michael R. Dufault, Paula Boutin, Dapei Liu, Mindy Zhang, Kristin Puorro-Radzwill, Lori Rulli, Dave Reczek, Rebecca Bagley, Ann Byrne, William Weber, Bruce Roberts, Katherine Klinger, William Brondyk, Mariana Nacht, Steve Madden, Robert Burrier, Srinivas Shankara, and Beverly A. Teicher

Genzyme Corp., Framingham, Massachusetts

Abstract

Protein tyrosine phosphatase PRL-3 mRNA was found highly expressed in colon cancer endothelium and metastases. We sought to associate a function with PRL-3 expression in both endothelial cells and malignant cells using *in vitro* models. PRL-3 mRNA levels were determined in several normal human endothelial cells exposed or unexposed to the phorbol ester phorbol 12-myristate 13-acetate (PMA) and in 27 human tumor cell lines. In endothelial cells, PRL-3 mRNA expression was increased in human umbilical vascular endothelial cells and human microvascular endothelial cells (HMVEC) exposed to PMA. An oligonucleotide microarray analysis revealed that PRL-3 was among the 10 genes with the largest increase in expression on PMA stimulation. Phenotypically, PMA-treated HMVEC showed increased invasion, tube formation, and growth factor-stimulated proliferation. A flow cytometric analysis of cell surface markers showed that PMA-treated HMVEC retained endothelial characteristics. Infection of HMVEC with an adenovirus expressing PRL-3 resulted in increased tube formation. In tumor cells, PRL-3 mRNA levels varied markedly with high expression in SKNAS neuroblastoma, MCF-7 and BT474 breast carcinoma, Hep3B hepatocellular carcinoma, and HCT116 colon carcinoma. Western blotting analysis of a subset of cell line lysates showed a positive correlation between PRL-3 mRNA and protein levels. PRL-3 was stably transfected into DLD-1 colon cancer cells. PRL-3-overexpressing DLD-1 subclones were assessed for doubling time and

invasion. Although doubling time was similar among parental, empty vector, and PRL-3 subclones, invasion was increased in PRL-3-expressing subclones. In models of endogenous expression, we observed that the MCF-7 cell line, which expresses high levels of PRL-3, was more invasive than the SKBR3 cell line, which expresses low levels of PRL-3. However, the MDA-MB-231 cell line was highly invasive with low levels of PRL-3, suggesting that in some models invasion is PRL-3 independent. Transfection of a PRL-3 small interfering RNA into MCF-7 cells inhibited PRL-3 expression and cell invasion. These results indicate that PRL-3 is functional in both endothelial cells and malignant cells and further validate PRL-3 as a potentially important molecular target for anticancer therapy. [Mol Cancer Ther 2006;5(2):219–29]

Introduction

The family of protein phosphatases of regenerating liver (PRL) comprises three members known as PRL-1, PRL-2, and PRL-3. Rat PRL-1 was originally identified as an immediate-early gene in regenerating liver (1). Murine PRL-2 and PRL-3 were subsequently discovered by amino acid sequence homology and display 87% and 76% sequence identity to murine PRL-1, respectively (2). All three PRL proteins contain a COOH-terminal prenylation motif (2). The human PRL-1, PRL-2, and PRL-3 have been elucidated more recently beginning with the description of human PRL-3 as a human muscle-specific tyrosine phosphatase (3–5).

Evidence is accumulating, suggesting that these proteins may be associated with oncogenic states. The first link between PRL expression and cancer comes from studies of tissue distribution showing widespread expression of PRL-1 in embryonic tissues. In the rat embryo, PRL-1 is expressed in the brain, intestine, liver, and esophageal epithelia. In the murine embryo, PRL-1 is expressed in the nervous and skeletal systems (6–9). Similarities between cancer cells and embryonic cells have been described in the literature, and the proposition has been made that neoplastic cells are dedifferentiated cells that have reverted to a state of embryonic plasticity (10–16). PRL-1 is elevated frequently in breast, ovarian, colon, prostate, and pancreatic cancers (17, 18).

An additional link between PRL proteins and cancer is the expression of PRL-1 in proliferative states. PRL-1 was isolated from regenerating liver, a physiologic process involving cell proliferation (1), which when deregulated may contribute to primary liver cancers (19). In addition, NIH3T3 cells transfected with PRL-1 display abnormal morphology and enhanced growth rate (1), whereas fibroblasts up-regulate PRL-1 mRNA expression on stimulation with serum (20). Consistent with these findings are

Received 7/29/05; revised 10/19/05; accepted 12/7/05.

The costs of publication of this article were defrayed in part by the payment of page charges. This article must therefore be hereby marked advertisement in accordance with 18 U.S.C. Section 1734 solely to indicate this fact.

Requests for reprints: Beverly A. Teicher, Genzyme Corp., 1 Mountain Road, Framingham, MA 01701. Phone: 508-271-2843; Fax: 508-620-1203. E-mail: Beverly.Teicher@Genzyme.com

Copyright © 2006 American Association for Cancer Research.

doi:10.1158/1535-7163.MCT-05-0289

those suggesting a role for PRL-1 in cell cycle regulation. Investigators have shown that the subcellular localization of endogenous PRL-1 was cell cycle dependent, with PRL-1 located in the endoplasmic reticulum of nonmitotic cells and to the centrosomes and spindle apparatus of mitotic cells (21, 22).

All three PRL proteins have been implicated directly in cancer progression. Overexpression of flag-tagged human PRL-1 protein in D27 hamster pancreatic ductal epithelial cells led to a loss of contact inhibition in culture and generated tumors in athymic nude mice (23). Similarly, human PRL-1 mRNA was shown to be up-regulated in benign prostatic fibroblast cells after stimulation with conditioned medium from the human prostate tumor cell line LNCaP and to be up-regulated in prostatic tumor fibroblast cells (22). PRL-1 mRNA was expressed in several tumor epithelial cell lines, including the HeLa cervical adenocarcinoma cell line, the HepG2 hepatoblastoma cell line, and a Burkitt's lymphoma cell line (1). PRL-2 mRNA overexpression was detected in prostate cancer cell lines and prostate tumor tissues (22). PRL-1 protein and PRL-3 protein were shown to increase cell motility and cell invasion *in vitro* (24–30). In the same study, PRL-3 protein was shown to be associated with dynamic membrane structures in an *in vitro* wound healing assay, and both PRL-1 and PRL-3 proteins induced metastasis in mice.

PRL-3 has been strongly implicated in human colon cancer progression. PRL-3 mRNA is a tumor endothelial marker expressed at higher levels in endothelial cells isolated from fresh specimens of human colon cancer than in endothelial cells isolated from normal colon mucosa (31, 32). PRL-3 mRNA was also shown to be expressed at higher levels in metastases of colorectal cancers compared with nonmetastatic tumors and normal colorectal epithelium (33). PRL-3 mRNA could not be detected in normal human colon tissue samples, in nonmetastatic colorectal carcinoma samples, or in lung and liver metastases of noncolorectal cancer origin. However, PRL-3 mRNA was detected in 4 of 4 colorectal cancer metastases to lymph nodes, 10 of 11 colorectal metastases to the liver, 6 of 7 colorectal metastases to the lung, 4 of 4 colorectal metastases to the brain, and 3 of 3 colorectal metastases to the ovary (34). These results show the selectivity of PRL-3 expression for colorectal cancer metastasis and suggest that PRL-3 may be an important mediator of the metastatic process in colon cancer.

We sought to associate a function with PRL-3 expression in both endothelial cells and malignant cells using *in vitro* models. In endothelial cell models, we show that PRL-3 expression is associated with increased tube formation, whereas in tumor cell models we show that PRL-3 expression is associated with increased invasiveness. Our data indicate that PRL-3 may be functional in both endothelial and malignant compartments of tumors and that it may play an important role in angiogenic, metastatic cancers.

Materials and Methods

Materials

PBS, fetal bovine serum (FBS), RPMI, penicillin/streptomycin, Versene, and G418 were purchased from Invitrogen, Inc. (Carlsbad, CA) Phorbol 12-myristate 13-acetate (PMA), DMSO, and protease inhibitor cocktail were purchased from Sigma Chemical Co. (St. Louis, MO). Basic fibroblast growth factor (bFGF) and vascular endothelial growth factor (VEGF) were purchased from R&D Systems, Inc. (Minneapolis, MN).

Cell Culture

All cells were grown at 37°C in 5% CO₂ humidified atmosphere. Human tumor cell lines, DLD-1 colon carcinoma (35, 36), SKNAS and IMR-32 neuroblastoma, and MCF-7, SKBR3, and MDA-MB-231 breast carcinoma (American Type Culture Collection, Manassas, VA) were grown in RPMI with 10% heat-inactivated FBS and 1% penicillin/streptomycin. Human umbilical vascular endothelial cells (HUVEC) and human microvascular endothelial cells (HMVEC; Cambrex, East Rutherford, NJ) were grown in EGM2-MV medium (Cambrex). Endothelial precursor cells (EPC) were derived from AC133⁺/CD34⁺ bone marrow cells (ref. 37; Cambrex) by exposure to 50 ng/mL VEGF, 10 to 50 ng/mL bFGF, and 5 units/mL heparin on fibronectin-coated flasks (Biocoat, Fort Washington, PA) in Iscove's modified Dulbecco's medium (Invitrogen) with 15% FBS. HMVEC, HUVEC, and EPC were exposed to 100 nmol/L PMA in DMSO in serum-free EBM2 (HUVEC and HMVEC) or serum-free Iscove's modified Dulbecco's medium (EPC) for 24 hours.

mRNA Extraction and Real-time Reverse Transcription-PCR

Total RNA was isolated by chloroform extraction using Trizol reagent (Invitrogen) and purified using Qiagen RNeasy method (Valencia, CA). Purified total RNA was subjected to formaldehyde gel electrophoresis and spectrophotometry ($A_{260\text{ nm}}$ and $A_{280\text{ nm}}$) to assess integrity and purity. Reverse transcription was done using cDNA Archive (Applied Biosystems, Foster City, CA). For quantification of PRL-3 mRNA, reverse transcription-PCR (RT-PCR) was done in duplicate on a 7700 real-time Taqman thermal cycler (Applied Biosystems) according to the manufacturer's instructions using 900 nmol/L primers (Integrated DNA Technologies, Coralville, IA), 250 nmol/L fluorogenic probe (Applied Biosystems), and Taqman Universal PCR Master Mix (Applied Biosystems). The forward primer sequence was 5'-ATCACCGTTGTG-GACTGGCC-3', the reverse primer sequence was 5'-CC-AGTCTTCCACTACCTTGCC-3', and the probe sequence was 5'-TTTGACGATGGGGCGCCCCCGC-3'. Loading was measured by 18S mRNA detection using rRNA Control Reagents (Applied Biosystems) in multiplex reactions with PRL-3 primers and probe. The 18S probe final concentration was 250 nmol/L and that of each 18S primer was 50 nmol/L. Absolute quantification of PRL-3 transcript copy number was done using a cDNA standard curve generated by serial dilution of a full-length human PRL-3 pcDNA plasmid (Invitrogen). Relative quantification

of PRL-3 mRNA was done according to the comparative cycle threshold method described by the Taqman manufacturer (Applied Biosystems). Control PCRs substituting water for cDNA were used as negative controls. Reverse transcription reactions were done both in the presence (RT+) and absence (RT-) of reverse transcriptase. RT- reactions were used as templates in the RT-PCR experiment to assess genomic DNA contamination in total RNA preparations and distinguish it from cDNA amplification. Most control RT-PCRs reached a cycle threshold of 40, reflecting absence genomic DNA contamination in the total RNA preparations and ensuring that the PCR products resulted from cDNA amplification. For PCR validation of the oligonucleotide microarray analysis of PMA-induced genes in HMVEC, RT-PCR was done on a 7900 real-time Taqman thermal cycler according to the manufacturer's instructions using SYBR Green PCR Master Mix (Applied Biosystems). Loading was measured by 18S mRNA detection using rRNA Control Reagents in singleplex reactions. Stanniocalcin-1 forward primer was GCTGGTGATCAGTGCTTCTGCAA and reverse primer was TTTGGGCCGCGCACTCGGGATTTC. Tissue inhibitor of matrix metalloproteinase-1 forward primer was ACAGACGGCCTTCTGCAATTC and reverse primer was TCATCTTGATCTCATAACGCTGGTA. Tissue factor pathway inhibitor-2 forward primer was TGTCACCGGAACCGGATTGA and reverse primer was TTAATAATAGCGAGTCACATTGG. Tissue-type plasminogen activator forward primer was CTGCCTCCCGTGGAAATTCATGA and reverse primer was AGCCCTCCTTTGATGCGAAA. CXCR-4 forward primer was GTGTCTCATCCTGGCCTTCAT and reverse primer was GGATCCAGACGCCAACATAG. Diacylglycerol kinase δ forward primer was GATGTGGTATGGAGTTCTTGGA and reverse primer was TGGGAATGTTAAGGACAGCAATT. Nidogen 2 forward primer was TTCCCGGCCATCGCCCCTTTTC and reverse primer was ACTTT-CCCATTAC-TCGGTACAG. Galanin forward primer was CCCGAGGACGCGCCCTCCTT and reverse primer was GGGTCCAGCCTCGTTTTTCCTT. Endothelial cell-specific molecule-1 forward primer was TGAGGTGTCAGCCTTCTAAT and reverse primer was GAAGGTGCCGTAGGGACAGT. All primers were synthesized by Integrated DNA Technologies. For the SYBR Green real-time PCR assay, the final primer concentration was 50 nmol/L to ensure the absence of nonspecific amplification. However, nidogen 2 could only be detected using 500 nmol/L primers. PCR products were run on a PAGE gel to verify size and confirm the absence of nonspecific bands. Expressed sequence tags were purchased from Invitrogen and used as positive controls.

Oligonucleotide Microarray Analysis

The gene expression of PMA-treated HMVEC 1F1645 and DMSO-treated HMVEC 1F1645 was compared. Total RNA was treated with DNase I (Ambion, Inc., Austin, TX), cleaned using Qiagen RNeasy protocol, and amplified using Ambion Amino Allyl MessageAmp Amplified RNA kit. Amplified RNAs were labeled with Cy3 or Cy5

dye. Labeled amplified RNAs were fragmented and hybridized on Agilent Human Oligo Microarray using Agilent hybridization kit (Palo Alto, CA). The experiment used reference design with universal human reference total RNA (Invitrogen) with dye swap. The images were quantified using Imagene 5.0 (Biodiscovery, Inc., Marina Del Rey, CA) imported to GeneSight 3.5 (Biodiscovery) for normalization and significance analysis. A *t* test was applied and genes were selected that had $P \leq 0.02$ (98% confidence).

Flow Cytometry

PMA-treated, DMSO-treated, and untreated HMVEC 1F1645 were suspended with Versene. Cells (10^5) were incubated in PBS/5% FBS with primary antibody (50 μ L, 1 hour) on ice. After washing, the cells were incubated with secondary antibody (1 hour), if necessary, on ice. After washing, the cells were suspended in cold buffer (300 μ L). Flow cytometry was conducted on a FACSCalibur (Becton Dickinson Labware, Franklin Lakes, NJ).

Primary antibodies to CD106, CD54, CD36 (FITC-labeled), CD105 (BD Biosciences, Franklin Lakes, NJ), CD31, VE-cadherin, VEGF receptor-2 (Santa Cruz Biotechnology, Inc., Santa Cruz, CA), and P1H12 (Chemicon International, Inc., Temecula, CA) were used at 5 μ g/mL, and the primary antibody to CD34 (FITC-labeled; BD Biosciences) was used at 3 μ g/mL. A FITC-labeled mouse IgG1 (BD Biosciences) was used as control for CD34 at 3 μ g/mL and as control for CD36 at 5 μ g/mL. Rabbit serum (Sigma) was used as a control for CD31 and VEGF receptor-2 at 5 μ g/mL. Goat serum (Sigma) was used as a control for VE-cadherin diluted 1:100. Purified mouse IgG1 (BD Biosciences) was used as a control for CD106, CD54, CD105, and P1H12 at 5 μ g/mL. Anti-mouse (Jackson ImmunoResearch Laboratories, Inc., West Grove, PA) was used with CD106, CD54, CD105, and P1H12 at 5 μ g/mL. Anti-rabbit (Jackson ImmunoResearch Laboratories) was used with CD31 and VEGF receptor-2 at 5 μ g/mL. Anti-goat (Santa Cruz Biotechnology) was used with VE-cadherin at 5 μ g/mL.

Western Blotting

Confluent cells in six-well plates were washed with cold PBS, and cold lysis buffer [50 μ L; EB buffer: 1% Triton, 20 mmol/L Tris-HCl (pH 7.4), 5 mmol/L EDTA, 10% glycerol, 150 mmol/L NaCl, 2 mmol/L sodium orthovanadate, protease inhibitor cocktail] was added on ice (5 minutes). Total cell lysates were collected with rubber scrapers, transferred to a 1.5 mL tube on ice, and then clarified by centrifugation (14,000 rpm, 20 minutes) at 4°C. Total protein concentration was determined by BCA Protein Assay kit (Pierce, Rockford, IL). Total cell lysates (250 μ g) were loaded onto a 4% to 12% Bis-Tris gel (Invitrogen) and run at 150 V (2 hours) using MES running buffer (Invitrogen). The protein was transferred onto a polyvinylidene difluoride membrane at 25 V (45 minutes) using a semidry transfer cell (Bio-Rad Laboratories, Hercules, CA) and then blocked for 1 hour to overnight with 5% dry milk in TBS with 0.01% Tween (Sigma). Anti-PRL-3 monoclonal antibody (no. 14; 1:500; a gift from Drs. Kinzler and

Vogelstein, Johns Hopkins University School of Medicine, Baltimore, MD) or anti-glyceraldehyde-3-phosphate dehydrogenase (1:6,000; Abcam, Cambridge, United Kingdom) was incubated for 1 hour. After washing, the membrane was incubated with horseradish peroxidase-labeled anti-mouse antibody (1:10,000; Jackson ImmunoResearch Laboratories) for 1 hour. After washing, the Western blot was developed using an enhanced chemiluminescence kit (Pierce). For the detection of PRL-3 inhibition in MCF-7 cells exposed to the PRL-3 small interfering RNA (siRNA), MCF-7 cells were transfected as described below (see PRL-3 siRNA Transfection). Total cell lysates (37 µg) were loaded onto a 4% to 12% Bis-Tris gel with MES buffer. Detection was achieved using an anti-PRL-3 rabbit polyclonal (Genesis Biotech, Inc. Taipei, Taiwan) diluted 1:2,000 and an anti-rabbit horseradish peroxidase-labeled secondary antibody (Jackson ImmunoResearch Laboratories) diluted 1:50,000. Detection was done using the Dura West detection system (Pierce).

Immunostaining

Cells were fixed with zinc/formaldehyde for 10 minutes, rinsed twice in PBS, and permeabilized with 0.2% Triton for 10 minutes. Image-iT FX signal enhancer (100 µL) was added for 30 minutes at room temperature. The cells were rinsed twice with PBS and anti-PRL-3 (Abcam) was added in blocking buffer (0.2% horse serum, 0.2% bovine serum albumin in PBS) for 1 hour at room temperature. After washing, a fluorochrome-labeled secondary antibody was added for 1 hour. The cells were then rinsed thrice with PBS. 4',6-Diamidino-2-phenylindole was counterstained and the slides were mounted with antifade.

PRL-3 Expression in DLD-1 Cells

Full-length PRL-3 cDNA (obtained from Drs. Kinzler and Vogelstein) was subcloned into pcDNA3.1/V5-His-TOPO vector (Invitrogen) expressing neomycin resistance gene, leaving the V5 and His tags out of frame. The pcDNA3.1/V5-His vector (Invitrogen) was the empty vector control. The PRL-3 construct and empty vector were transfected separately and stably into DLD-1 cells using Lipofectamine 2000 reagent (Invitrogen). Stably transfected DLD-1 cells were subcloned by limiting dilution and propagated in RPMI with 10% heat-inactivated FBS and 500 µg/mL G418.

PRL-3 Expression in HMVEC

PRL-3-expressing adenovirus was made using the AdEasy XL Adenoviral Vector System (Stratagene, La Jolla, CA). The plasmid construct pcDNA3-V5-HIS-PRL3 was digested with *KpnI* and *EcoRV* (New England Biolabs, Beverly, MA) and the 596-bp insert was gel isolated. The insert was ligated into the *KpnI* and *EcoRV* sites of pShuttle-CMV (Stratagene). The construct pShuttle-CMV-PRL3 was then linearized with *PmeI* (New England Biolabs) and transformed into electrocompetant BJ5183-Ad-1 cells (Stratagene) according to the manufacturer's directions. Recombinant pAd-CMV-PRL3 plasmid DNA was prepared and recombination was verified with a *PacI* digest. *PacI*-digested recombinant Ad plasmid was then transfected into Ad293 cells (Stratagene) using Lipofectamine 2000. When the transfected Ad293 cells reached

complete CPE, the cells were resuspended in a small volume of PBS and freeze thawed thrice. The lysed cells were then spun down and the supernatant was taken as Ad-CMV-PRL3 primary viral stock. HMVEC 1F1645 were infected with 50 multiplicities of infection of the primary viral stock and functionally assayed 48 hours postinfection.

PRL-3 siRNA Transfection

PRL3-DLD1-IIG5 and MCF-7 cells were grown in RPMI with 10% FBS, 1% penicillin/streptomycin, and 500 µg/mL G418. The cells (5×10^4 per well) were plated in a 24-well plate in medium without antibiotics 24 hours before transfection. All transfections were carried out in triplicate. The protocol for siRNA transfection in a 24-well format (Invitrogen) was followed for all transfections. The general procedure is as follows: (a) siRNA (20 pmol; 1 µL of a 20 µmol/L solution) was added to 50 µL Opti-MEM I reduced serum medium, (b) Lipofectamine 2000 (1 µL) was added to 50 µL Opti-MEM I reduced serum medium and incubated for 5 minutes at room temperature, (c) The siRNA and Lipofectamine were mixed and incubated at room temperature for 20 minutes, and (d) The 100 µL mixture was added to the cells. The siRNAs used were siRNA Negative-1 (Ambion), siRNA against lamin A/C (Xeragon/Qiagen, Valencia, CA; target sequence: AACTGGACTTCCAGAAGAACA), and siRNA against PRL-3 (Xeragon/Qiagen; target sequence: TGA-GAGCGGGATGAAGTACGA). Following the 48-hour incubation at 37°C, RNA for Taqman analysis was isolated using Trizol and pooled.

Proliferation Assay

Endothelial cells (5×10^3) in triplicate in a 96-well plate were incubated with various VEGF and bFGF concentrations in the presence or absence of 100 nmol/L PMA or 0.00125% DMSO at 37°C in a 5% CO₂ humidified atmosphere for 96 hours. Tumor cells (2×10^3) in duplicate in a 96-well plate were incubated at 37°C in RPMI with 2% heat-inactivated FBS in a 5% CO₂ humidified atmosphere for 96 hours. Proliferation was measured using CellTiter-Glo reagent (Promega, Madison, WI) on a microplate luminometer and Winglow software (Berthold Tech, Bad Wildbad, Germany).

Endothelial Cell Tube Formation Assay

Cells (2×10^4) were seeded in triplicate in a 96-well plate precoated with Matrigel (Becton Dickinson Labware) in serum-free EBM2 with 20 ng/mL each of bFGF and VEGF and in the presence or absence of 100 nmol/L PMA or 0.00125% DMSO at 37°C in a 5% CO₂ humidified atmosphere for 4 hours. After 24 hours, the cells were stained in 4 µg/mL calcein (Molecular Probes, Eugene, OR) in PBS at 37°C, imaged, and quantified using the image analysis software Scion Image (Scion Corp., Frederick, MD).

Invasion Assays

A modified Boyden chamber 24-well Transwell with fluoroblock inserts precoated with Matrigel (ref. 38; BD Biosciences) was used. Cells (2.5×10^4) were seeded per insert in duplicate in 500 µL serum-free medium. Inserts were placed in wells containing 500 µL medium with 5%

FBS. When appropriate, PMA was added to both chambers. The cells were incubated (48 hours) at 37°C in 5% CO₂ humidified atmosphere and the inserts were placed in a 24-well plate containing 500 µL calcein (4 µg/mL, 1 hour) in PBS at 37°C. Fluorescence was read on a Cytofluor II fluorescence plate reader (PerSeptive Biosystems, Foster City, CA) with excitation/emission wavelengths of 530/590 nm.

Statistical Analysis

Analysis of statistical significance was done using *t* tests for assays consisting of two experimental sample groups. The ANOVA test and Tukey-Kramer *post hoc* test were used to determine statistical significance in assays consisting of more than two experimental sample groups.

Results

PRL-3 mRNA expression was examined by real-time RT-PCR in human normal endothelial cells and in 27 human tumor cell lines (Fig. 1). HMVEC, HUVEC, and EPC were

examined for PRL-3 mRNA expression without treatment or after exposure to PMA (100 nmol/L, 24 hours). Under standard conditions, all endothelial cells had <1,000 transcripts of PRL-3 mRNA per reaction. Four of five endothelial cells tested [lung HMVEC, HMVEC 1F1645 (neonatal dermal), HMVEC OF1025 (neonatal dermal), and HUVEC] had a marked increase in PRL-3 mRNA after exposure to PMA. PRL-3 mRNA was increased 27-, 23-, 11-, and 23-fold in the lung HMVEC, HMVEC 1F1645, HMVEC OF1025, and HUVEC, respectively, by exposure to PMA compared with DMSO. HMVEC 1F1645 was most responsive to PMA with an average of 14,428 transcripts per reaction after PMA exposure compared with 500 without PMA exposure.

Twenty-seven human tumor cell lines were evaluated by real-time RT-PCR for expression of PRL-3 mRNA (Fig. 1). The four human melanoma cell lines had low levels of PRL-3 mRNA. All three neuroblastoma cell lines expressed relatively high levels of PRL-3 mRNA ranging from an average of 1,252 transcripts per reaction in the IMR-32 cell line to an average of 21,969 transcripts per

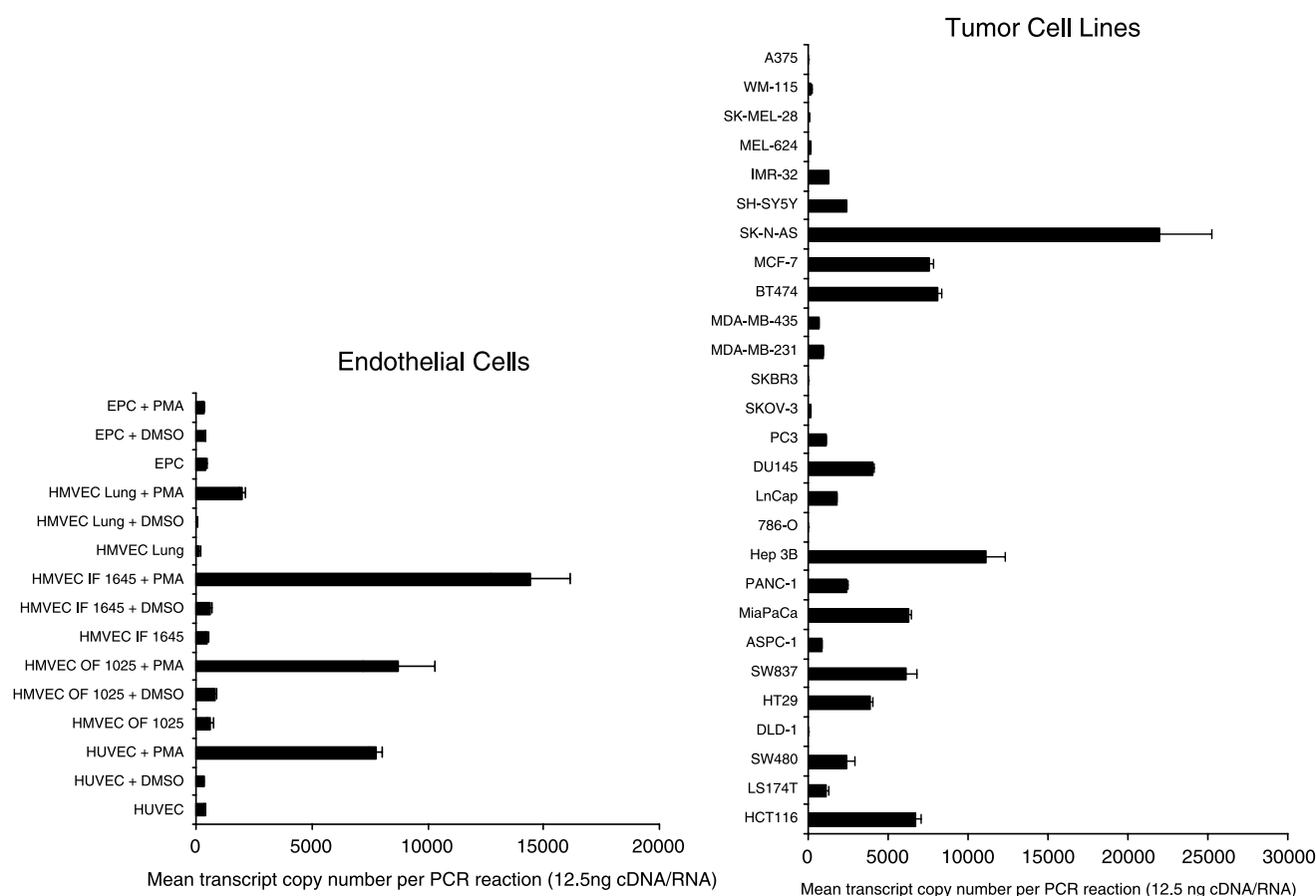


Figure 1. RT-PCR analysis of PRL-3 mRNA showing expression in normal human endothelial cells in the presence and absence of PMA exposure in EPC, HMVEC lung, HMVEC 1F1645, HMVEC OF1025, and HUVEC and expression in human tumor cell lines. A cycle threshold of 40 (no signal) was obtained in control PCRs where water was substituted for cDNA (data not shown). Control PCRs using mock reverse transcription reactions as templates (reactions where water had been substituted for reverse transcriptase) indicated negligible genomic DNA contamination (data not shown).

reaction in the SKNAS cell line. The five human breast cancer cell lines had varied expression of PRL-3 mRNA ranging from an average of 31 transcripts per reaction in the SKBR3 breast adenocarcinoma cell line to averages of 7,571 and 8,082 transcripts per reaction in the MCF-7 breast adenocarcinoma and BT474 breast carcinoma cell lines, respectively. The SKOV3 ovarian adenocarcinoma cell line had low expression of PRL-3 mRNA with an average of 187 transcripts per reaction. All three prostate cancer cell lines tested had relatively high levels of PRL-3 mRNA with averages of 1,125, 4,067, and 1,795 transcripts per reaction, respectively. The 786-O renal cell adenocarcinoma cell line had negligible levels of PRL-3 mRNA. The Hep3B hepatocellular carcinoma cell line had high levels of PRL-3

mRNA with an average of 11,163 transcripts per reaction. The three pancreatic cancer cell lines were positive for PRL-3 mRNA with averages of 866, 2,371, and 6,310 transcripts per reaction, respectively. The six colorectal cancer cell lines had varied PRL-3 mRNA ranging from negligible amounts of PRL-3 transcripts with an average of a single transcript per reaction in the DLD-1 colorectal adenocarcinoma cell line to an average of 6,752 and 6,108 transcripts per reaction in the HCT116 colorectal carcinoma and SW837 rectal adenocarcinoma cell lines, respectively.

Exposure to PMA did not alter expression of cell surface markers on HMVEC 1F1645, including P1H12, VEGF receptor-2, VE-cadherin, CD105, CD34, CD31, CD36, CD54, and CD106 as determined by flow cytometry (data

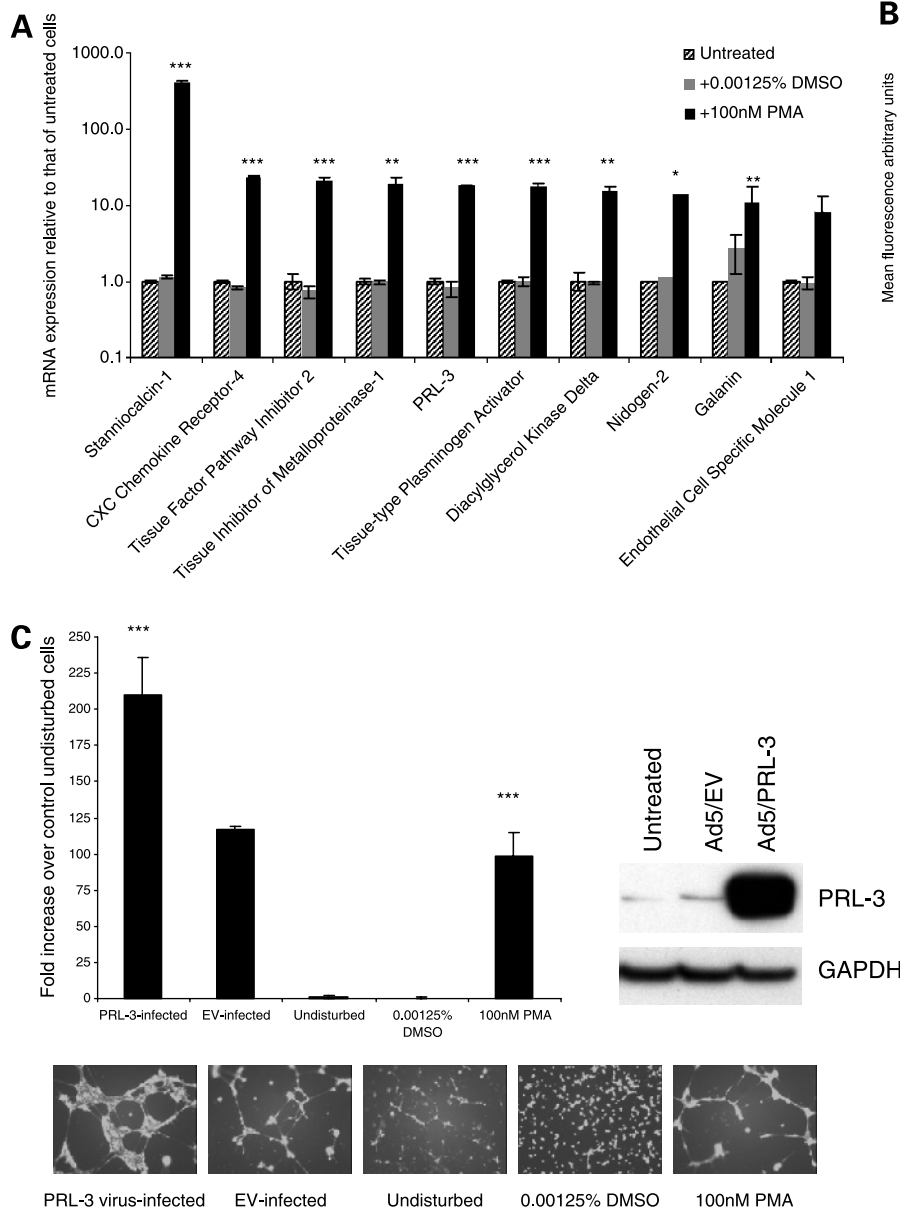


Figure 2. **A**, PMA-induced HMVEC 1F1645 gene expression by RT-PCR. mRNA levels relative to untreated cells. **B**, relative invasion by HMVEC 1F1645 in the presence and absence of PMA exposure. Representative experiment. **C**, tube formation by HMVEC 1F1645 in the presence and absence of PMA exposure and after infection with either PRL-3-expressing adenovirus or empty adenovirus. Data are compared with undisturbed cells (untreated and uninfected). Representative experiment. Western blot showing PRL-3 protein levels in infected HMVEC 1F1645. ***, $P < 0.001$; **, $P < 0.01$; *, $P < 0.05$ versus control cells.

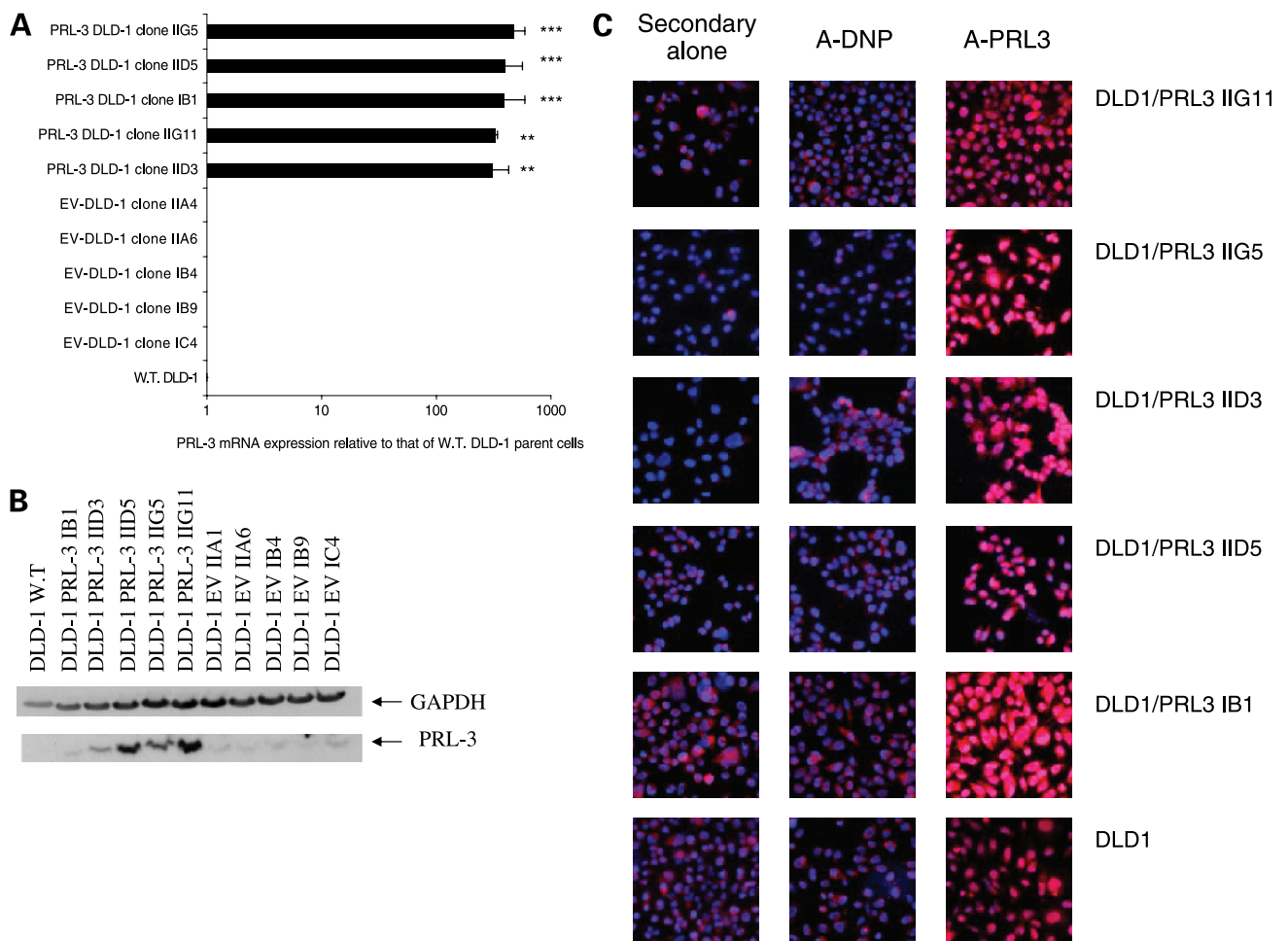


Figure 3. **A**, RT-PCR assay showing PRL-3 mRNA in five DLD-1 subclones transfected with a vector containing PRL-3 cDNA, five DLD-1 subclones transfected with empty vector, and parental DLD-1 cells. **B**, Western blot showing PRL-3 protein in five DLD-1 subclones transfected with a vector containing PRL-3 cDNA, five DLD-1 subclones transfected with empty vector, and parental DLD-1 cells. **C**, immunostaining showing the PRL-3 protein in five DLD-1 subclones transfected with a vector containing PRL-3 cDNA and parental DLD-1 cells. Representative experiment. ***, $P < 0.001$; **, $P < 0.01$ versus control cells.

not shown). However, exposure to PMA (100 nmol/L) enhanced proliferation of HMVEC 1F1645 in the absence of and over a concentration range of VEGF and bFGF (up to 20 ng/mL each; data not shown).

The invasion activity of HMVEC 1F1645 was assessed in the presence or absence of 100 nmol/L PMA. Exposure to PMA increased the invasiveness of the cells by ~4-fold compared with untreated controls and ~6-fold compared with DMSO-treated cells (Fig. 2). For tube formation assays, HMVEC 1F1645 were treated with either 0.00125% DMSO or 100 nmol/L PMA in the presence of bFGF and VEGF (20 ng/mL each). PMA exposure increased tube area compared with both controls (Fig. 2).

The effect of PMA (100 nmol/L, 24 hours) on HMVEC gene expression was assessed by oligonucleotide microarray analysis and subsequent RT-PCR analysis. The most highly up-regulated mRNAs were stanniocalcin-1, CXCR-4, tissue factor pathway inhibitor-2, tissue inhibitor

of matrix metalloproteinase-1, PRL-3, tissue-type plasminogen activator, diacylglycerol kinase δ , nidogen-2, galanin, and endothelial cell-specific molecule-1 (Fig. 2). Infection of HMVEC 1F1645 with a PRL-3-containing adenovirus increased tube formation compared with infection with an empty adenovirus or lack of infection, showing that PRL-3 up-regulation can promote tube formation (Fig. 2).

Total RNA was isolated from parental DLD-1 colon cancer cells and DLD-1 subclones transfected with empty vector or PRL-3-containing plasmid vector, and cDNA was prepared and analyzed for PRL-3 mRNA by RT-PCR. Five empty vector-transfected DLD-1 subclones and five PRL-3-transfected subclones were selected for characterization (Fig. 3). Protein from the subclones and parental cells was analyzed by Western blotting with a mouse monoclonal anti-PRL-3 and by immunostaining with a goat polyclonal anti-PRL-3 to determine PRL-3 protein expression. Western

blot analysis showed the highest PRL-3 protein in subclones PRL3-IIG11 and PRL3-IID5, moderate PRL-3 in subclone PRL3-IIG5, and lower PRL-3 in subclones PRL3-IID3 and PRL3-IB1. Parental DLD-1 and empty vector-transfected subclones have very low to undetectable PRL-3 protein (Fig. 3). Immunostaining showed low PRL-3 protein in parental cells, moderate PRL-3 protein in subclones PRL3-IIG11 and PRL3-IID5, and high PRL-3 protein in subclones PRL3-IIG5, PRL3-IID3, and PRL3-IB1 (Fig. 3). The differences in PRL-3 obtained by Western blotting and immunostaining may reflect differences in the antibodies used because both antibodies cross-react with the PRL-2 protein.

Generation times were determined for the five PRL-3-expressing DLD-1 subclones, five empty vector-transfected DLD-1 subclones, and parental DLD-1 cells (Fig. 4). The PRL-3 protein level was not associated with generation time, because the population doubling time of the five PRL-3-expressing subclones (18.5 hours in 10% FBS and 38 hours in 2% FBS), the five empty vector-transfected subclones (14.4 hours in 10% FBS and 33.3 hours in 2% FBS), and the parental DLD-1 cells (11.5 hours in 10% FBS and 25.3 hours in 2% FBS) were similar. The five PRL-3-expressing subclones, five empty vector-transfected subclones, and parental DLD-1 cells were assayed for invasion through Matrigel. The PRL-3-expressing DLD-1 subclones invasiveness was 2-fold greater than that of the parental cells, whereas the empty vector-transfected subclones invasiveness was 2-fold less than that of the parental cells (Fig. 4).

When human breast cancer cell lines endogenously expressing high or low levels of PRL-3 protein (Fig. 5) were assayed for invasion through Matrigel, the MCF-7 breast adenocarcinoma cell line was more invasive than the SKBR3 breast adenocarcinoma cell line. However, the MDA-MB-231 breast adenocarcinoma cell line (low PRL-3 mRNA and protein) was as invasive as the MCF-7 cell line (high PRL-3 mRNA and protein). Therefore, there was a trend between PRL-3 and invasion through Matrigel with two of three human tumor cell lines (Fig. 6). MCF-7 cells transfected with a PRL-3 siRNA had decreased levels of PRL-3 mRNA and protein (Fig. 5) and a reduced ability to invade through Matrigel at 72 hours post-transfection (Fig. 6).

Discussion

Phosphatases involved in critical aspects of malignant disease could be interesting drug targets. PRL-3 mRNA was detectable in a broad range of human tumor cell lines and endothelial cells. These data reinforce and expand on previously published results, indicating that PRL-3 is expressed in the epithelial and endothelial compartments of tumors (31–34, 39, 40).

The expression of PRL-3 mRNA was highly variable among the primary tumor-derived colorectal cancer cell lines, SW837, HT29, DLD-1, SW480, LS174T, and HCT116 (Fig. 1; refs. 35, 36, 41–44). Using clinical tissues, Saha et al.

(33) and Bardelli et al. (34) found higher levels of PRL-3 mRNA in colorectal tumor metastases compared with the primary tumor from the same patient. Our findings suggest that advanced primary tumors may express higher PRL-3 mRNA levels than lower grade tumors. Cell lines with moderate PRL-3 mRNA, such as HT29, SW480, and LST174T colorectal adenocarcinomas, or with high PRL-3 mRNA, such as SW837 rectal adenocarcinoma and HCT116 colorectal carcinoma, might have been derived from primary tumors that had developed a metastatic phenotype. Indeed, Leibovitz et al. (43) stated that the SW480 line was derived from a Duke's class B primary tumor, indicating that the primary tumor had invaded the muscularis propria of the bowel wall. Leibovitz et al. (43)

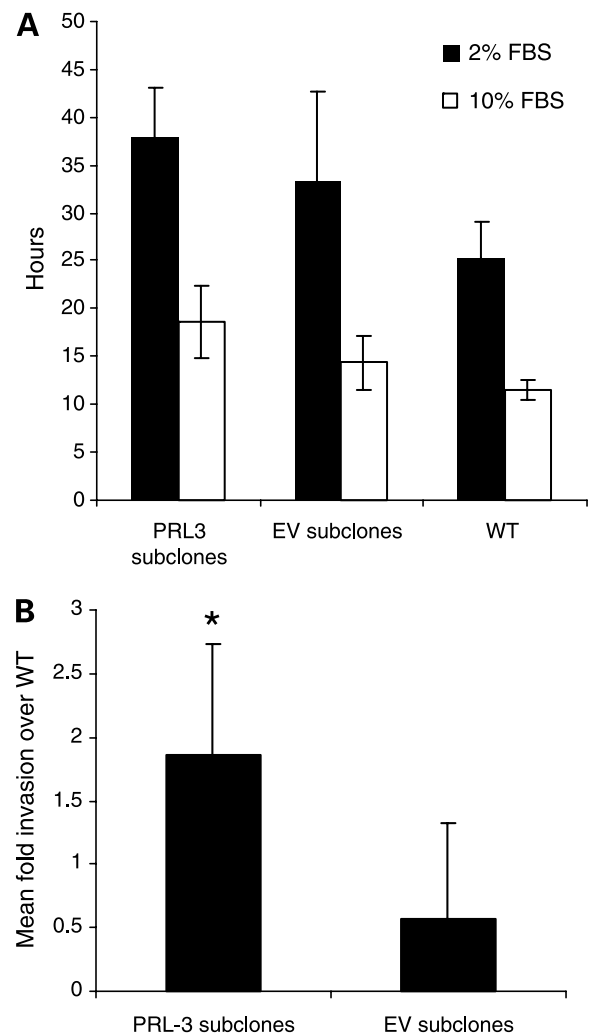


Figure 4. **A**, mean generation times obtained for five PRL-3-expressing subclones, five empty vector-transfected subclones, and parental DLD-1 cells determined in 2% or 10% FBS. *Columns*, mean of two independent experiments; *bars*, SD. **B**, relative mean invasion obtained for five PRL-3-expressing subclones and five empty vector-transfected subclones compared with parental DLD-1 cells. *Columns*, mean of three independent experiments; *bars*, SD. *, $P < 0.05$ versus control cells.

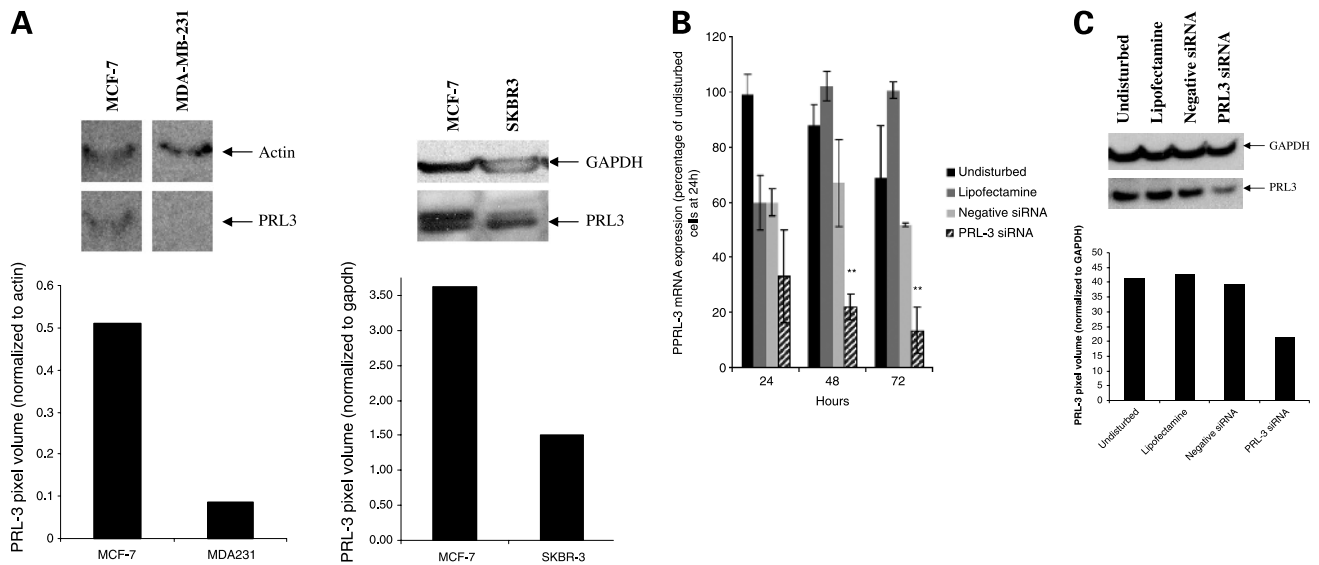


Figure 5. **A**, Western blots showing PRL-3 protein levels in three human breast adenocarcinoma cell lines that express PRL-3 endogenously. **B**, RT-PCR analysis of PRL-3 mRNA in MCF-7 cells exposed to PRL-3 siRNA 72 h post-transfection. **C**, Western blot showing PRL-3 protein levels in MCF-7 cells exposed to PRL-3 siRNA 72 h post-transfection. **, $P < 0.01$ versus control cells.

also reported that cancer recurred a year later with widespread metastasis in the same patient. Similarly, the SW837 line was derived from a Duke's class C rectal tumor, indicating that the tumor had invaded the regional lymph node (43). In addition, the HCT116 line, a high expresser of PRL-3 mRNA, is a poorly differentiated and aggressive cell line, a characteristic consistent with advanced cancer stages.

In noncolorectal cancer cell lines, high PRL-3 mRNA expression was observed in cells derived from primary tumors, such as the Hep3B hepatocellular carcinoma line (45), and metastases, such as the SKNAS neuroblastoma line, derived from a bone marrow metastasis (46), and the MCF-7 mammary carcinoma line, derived from a pleural effusion (47). Thus, in addition to colorectal cancers, PRL-3 may play a broad role in cancer. The low levels or absence of PRL-3 mRNA expression in melanoma lines suggested that PRL-3 might not be a prominent factor in skin cancers (Fig. 1).

PRL-3 mRNA was low in endothelial cells but was increased in HMVEC from several donors on PMA exposure (Fig. 1). PMA-treated HMVEC retained an endothelial phenotype as determined by surface markers. On PMA exposure, HMVEC 1F1645 increased proliferation, invasion, and tube formation, phenotypes related to malignancy and angiogenesis (Fig. 2). Characterization of mRNA isolated from PMA-treated HMVEC 1F1645 by oligonucleotide microarray and PCR analysis indicated that exposure to PMA stimulated the expression of many genes associated with cancer (Fig. 2). The most highly up-regulated gene on PMA exposure was stanniocalcin-1, a gene recently identified as a molecular blood and bone marrow marker for human breast cancer (48). Tissue inhibitor of matrix metalloproteinase-1, another gene up-

regulated on PMA exposure, is overexpressed in pancreatic cancer (49) and papillary thyroid carcinoma (50) and was shown to correlate with poor prognosis in renal cell carcinoma (51). Tissue factor pathway inhibitor-2, which was induced by PMA, was shown to be expressed at higher levels in aggressive human melanoma lines than in poorly aggressive lines (52). These data strengthen the conclusion in HMVEC 1F1645 that PMA exposure results in molecular and cellular phenotypes like malignancy. PRL-3 was among highly up-regulated genes on PMA exposure strengthening the notion that PRL-3 may be a driver for tumor-supportive endothelial phenotypes (Fig. 2). HMVEC 1F1645 infection with an adenovirus expressing PRL-3 allowed the increased expression of PRL-3 in the absence of other alterations attributable to PMA exposure and resulted in increased tube formation by the HMVEC, suggesting that high PRL-3 levels in endothelial cells may be associated with tumor angiogenesis (32).

Saha et al. (33) and Bardelli et al. (34) found PRL-3 overexpressed in colorectal cancer metastases. To model high PRL-3 levels in a cell-based assay system, the human colorectal adenocarcinoma cell line DLD-1, which endogenously expressed very low PRL-3 mRNA and protein, was selected (Fig. 1). After transfection, five DLD-1 subclones stably expressing PRL-3 mRNA were used for phenotypic characterization (Fig. 3). Parental DLD-1 cells and five subclones stably expressing empty vector were used as controls. PRL-3 protein levels in the DLD-1 PRL-3 and empty vector subclones and the parental cells were determined by Western blot and by immunostaining. Subclones PRL3-IIG11, PRL3-IID5, and PRL3-IIG5 showed the highest levels of PRL-3 protein by Western blot, whereas subclones PRL3-IIG5, PRL3-IID3, and PRL3-IB1 were the highest expressers by immunostaining (Fig. 3).

The differences may be due to cross-reactivity of the antibodies with PRL-2 protein. The ranking of the subclones based on ability to invade through Matrigel was PRL3-IIG5 > PRL3-IID3 and PRL3-IB1 > PRL3-IIG11 > PRL3-IID5, which is in close agreement with the immunostaining results for PRL-3 protein (Fig. 3). The generation time for each of the subclones and parental DLD-1 cells indicated that PRL-3 expression was not associated with proliferation rate (Fig. 4). However, invasion assays showed that higher PRL-3 expression was associated with increased invasion.

Invasion assays were subsequently done with human tumor cell lines with high and low endogenous PRL-3, including three human breast adenocarcinoma cell lines. The MCF-7 breast adenocarcinoma line, a high PRL-3 expresser, was more invasive than the SKBR3 breast adenocarcinoma line, a low PRL-3 expresser. However,

the MDA-MB-231 breast adenocarcinoma line, a low PRL-3 mRNA and protein expresser, was as invasive as the MCF-7 cell line (Figs. 1, 5, and 6). Overall, for two of three human tumor cell lines, there was a trend toward high PRL-3 expression and greater invasiveness, supporting a role for PRL-3 in invasion (2). However, the MDA-MB-231 breast adenocarcinoma line, which has low PRL-3 mRNA and protein levels, had robust invasion through Matrigel, indicating that PRL-3 expression is not required for invasion by all cells. Conclusive demonstration that PRL-3 actively promotes invasiveness in breast cancer cell lines was achieved by transfecting MCF-7 cells with a PRL-3 siRNA. MCF-7 cells exposed to the PRL-3 siRNA showed decreased PRL-3 mRNA and protein levels 72 hours post-transfection and reduced invasion through Matrigel (Figs. 5 and 6).

PRL-3, originally identified as a phosphatase in regenerating liver, continues to be validated as a potentially interesting drug target in malignant disease. PRL-3 has been found to be up-regulated in tumor endothelium and in metastatic colon cancer cells preclinically and clinically (31–34, 39). PRL-3 is up-regulated by exposure of endothelial cells to PMA and can be directly implicated in increased tube formation by PRL-3 adenovirus-infected HMVEC and in invasion by stably transfected DLD-1 subclones and endogenously expressing tumor cell lines. PRL-3 represents both an antiangiogenic and an antitumor target in malignant disease (53).

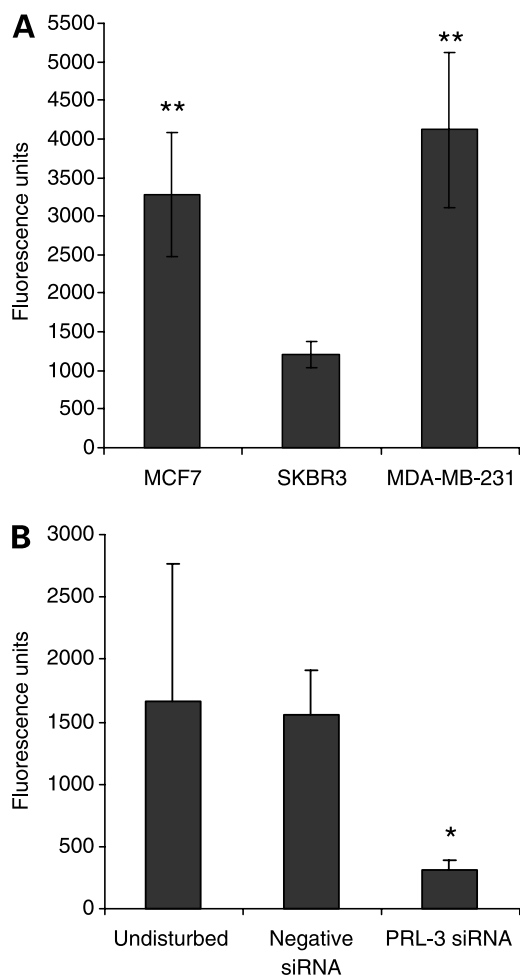


Figure 6. **A**, relative invasion by human tumor cell lines, including MCF-7, SKBR3, and MDA-MB-231 breast adenocarcinomas that express PRL-3 endogenously. *Columns*, mean of two independent experiments; *bars*, SD. **B**, relative invasion by MCF-7 cells exposed to PRL-3 siRNA 72 h post-transfection. **, $P < 0.01$ for MCF-7 and MDA-MB-231 compared with SKBR3.

References

- Diamond RH, Cressman DE, Laz TM, Abrams CA, Taub R. PRL-1, a unique nuclear protein tyrosine phosphatase, affects cell growth. *Mol Cell Biol* 1994;14:3752–62.
- Zeng Q, Hong W, Tan YH. Mouse PRL-2 and PRL-3, two potentially prenylated protein tyrosine phosphatases homologous to PRL-1. *Biochem Biophys Res Commun* 1998;244:421–7.
- Matter WF, Estridge T, Zhang C, et al. Role of PRL-3, a human muscle-specific tyrosine phosphatase, in angiotensin-II signaling. *Biochem Biophys Res Commun* 2001;283:1061–8.
- Zhou H, Gallina M, Mao H, et al. ^1H , ^{13}C and ^{15}N resonance assignments and secondary structure of the human protein tyrosine phosphatase, PRL-2. *J Biomol NMR* 2003;27:397–8.
- Pathak MK, Dhawan D, Lindner DJ, Borden EC, Farver C, Yi T. Pentamidine is an inhibitor of PRL phosphatases with anticancer activity. *Mol Cancer Ther* 2002;1:1255–64.
- Haber B, Najji L, Cressman D, Taub R. Coexpression of liver-specific and growth-induced genes in perinatal and regenerating liver: attainment and maintenance of the differentiated state during rapid proliferation. *Hepatology* 1995;22:906–14.
- Takano S, Fukuyama M, Kimura J, Xue J, Ohashi H, Fujita J. PRL-1, a protein tyrosine phosphatase, is expressed in neurons and oligodendrocytes in the brain and induced in the cerebral cortex following transient forebrain ischemia. *Brain Res Mol Brain Res* 1996;40:105–15.
- Rundle CH, Kappen C. Developmental expression of the murine PRL-1 protein tyrosine phosphatase gene. *J Exp Zool* 1999;283:612–7.
- Kong W, Swain GP, Li S, Diamond RH. PRL-1 PTPase expression is developmentally regulated with tissue-specific patterns in epithelial tissues. *Am J Physiol Gastrointest Liver Physiol* 2000;279:G613–21.
- Chodosh LA. Expression of BRCA1 and BRCA2 in normal and neoplastic cells. *J Mammary Gland Biol Neoplasia* 1998;3:389–402.
- Ito T, Noguchi Y, Udaka N, Kitamura H, Satoh S. Glucose transporter

- expression in developing fetal lungs and lung neoplasms. *Histol Histo-pathol* 1999;14:895–904.
12. Waltzer L, Bienz M. The control of β -catenin and TCF during embryonic development and cancer. *Cancer Metastasis Rev* 1999;18:231–46.
 13. Krupp G, Bonatz G, Parwaresch R. Telomerase, immortality and cancer. *Biotechnol Annu Rev* 2000;6:103–40.
 14. Meszoely IM, Means AL, Scoggins CR, Leach SD. Developmental aspects of early pancreatic cancer. *Cancer J* 2001;7:242–50.
 15. Teicher BA. Malignant cells, directors of the malignant process: role of transforming growth factor- β . *Cancer Metastasis Rev* 2001;20:133–43.
 16. Sood AK, Fletcher MS, Hendrix MJ. The embryonic-like properties of aggressive human tumor cells. *J Soc Gynecol Investig* 2002;9:2–9.
 17. Werner SR, Lee PA, Cummings OW, Randall SK, Crowell DN, Crowell PL. PRL-1 protein tyrosine phosphatase accelerates progression into S phase and is found at elevated levels in human ovarian, breast, pancreatic, colon and prostate cancers [abstract 818]. *Proc Amer Assoc Cancer Res 95th Annu Meet* 2004.
 18. Stephens BJ, Farnsworth AL, Munoz RM, et al. Lipid phosphatase activity of PRL-1 [abstract 865]. *Proc Amer Assoc Cancer Res 95th Annu Meet* 2004.
 19. Diehl AM. Liver regeneration. *Front Biosci* 2002;7:301–14.
 20. Diamond RH, Peters C, Jung SP, et al. Expression of PRL-1 nuclear PTPase is associated with proliferation in liver but with differentiation in intestine. *Am J Physiol* 1996;271:G121–9.
 21. Wang J, Kirby CE, Herbst R. The tyrosine phosphatase PRL-1 localizes to the endoplasmic reticulum and the mitotic spindle and is required for normal mitosis. *J Biol Chem* 2002;277:46659–68.
 22. Wang Q, Holmes DIR, Powell SM, Lu QL, Waxman J. Analysis of stromal-epithelial interactions in prostate cancer identifies PTPCAAX2 as a potential oncogene. *Cancer Lett* 2002;175:63–9.
 23. Cates CA, Michael RL, Stayrook KR, et al. Prenylation of oncogenic human PTP(CAAX) protein tyrosine phosphatases. *Cancer Lett* 1996;110:49–55.
 24. Zeng Q, Dong J-M, Guo K, et al. PRL-3 and PRL-1 promote cell migration, invasion and metastasis. *Cancer Res* 2003;63:2716–22.
 25. Gou K, Li J, Tang JP, Koh V, Gan BQ, Zeng Q. Catalytic domain of PRL-3 plays an essential role in tumor metastasis: formation of PRL-3 tumors inside the blood vessels. *Cancer Biol Ther* 2004;3:945–51. Epub 2004 Oct 27.
 26. Miskad UA, Semba S, Kato H, Yokozaki H. Expression of PRL-3 phosphatase in human gastric carcinomas: close correlation with invasion and metastasis. *Pathobiology* 2004;71:176–84.
 27. Wu X, Zeng H, Zhang X, et al. Phosphatase regenerating liver-3 promotes motility and metastasis of mouse melanoma cells. *Am J Pathol* 2004;164:2039–54.
 28. Peng L, Ning J, Meng L, Shou C. The association of the expression level of protein tyrosine phosphatase PRL-3 protein with liver metastasis and prognosis of patients with colorectal cancer. *J Cancer Res Clin Oncol* 2004;130:521–6.
 29. Lim KA, Song JS, Jee J, et al. Structure of human PRL-3, the phosphatase associated with cancer metastasis. *FEBS Lett* 2004;565:181–7.
 30. Kozlov G, Cheng J, Ziomek E, Banville D, Gehring K, Ekiel I. Structural insights into molecular function of the metastasis-associated phosphatase PRL-3. *Biol Chem* 2004;279:11882–9.
 31. Sager J, Benvenuti S, Bardelli A. PRL-3: a phosphatase for metastasis? *Cancer Biol Ther* 2004;3:952–3. Epub 2004 Oct 8.
 32. St. Croix B, Rago C, Velculescu V, et al. Genes expressed in human tumor endothelium. *Science* 2000;289:1197–202.
 33. Saha S, Bardelli A, Buckhaults P, et al. A phosphatase associated with metastasis of colorectal cancer. *Science* 2001;294:1343–6.
 34. Bardelli A, Saha S, Sager J, et al. PRL-3 expression in metastatic cancers. *Clin Cancer Res* 2003;9:5607–13.
 35. Dexter DL, Spremulli EN, Fligiel Z, et al. Heterogeneity of cancer cells from a single human colon carcinoma. *Am J Med* 1981;71:949–56.
 36. Dexter DL. *N,N*-dimethylformamide-induced alteration of cell culture characteristics and loss of tumorigenicity in cultured human colon carcinoma cells. *Cancer Res* 1979;39:1020.
 37. Bagley R, Walter-Yohrling J, Cao X, et al. Endothelial precursor cells as a model of tumor endothelium: characterization and comparison to mature endothelial cells. *Cancer Res* 2003;63:5866–73.
 38. Grotendorst GR. Spectrophotometric assay for the quantitation of cell migration in the Boyden chamber chemotaxis assay. *Methods Enzymol* 1987;147:144–52.
 39. Peng Y, Du K, Ramirez S, Diamond RH, Taub R. Mitogenic up-regulation of the PRL-1 protein-tyrosine phosphatase gene by Erg-1: EGR-1 activation is an early event in liver regeneration. *J Biol Chem* 1999;274:4513–20.
 40. Peng L, Ning J, Meng L, Shou C. The association of the expression level of protein tyrosine phosphatase PRL-3 protein with liver metastasis and prognosis of patients with colorectal cancer. *J Cancer Res Clin Oncol* 2004;130:521–6. Epub 2004 May 6.
 41. Von Kleist S, Chany E, Burtin P, King M, Fogh J. Immunohistology of the antigenic pattern of a continuous cell line from a human colon tumor. *J Natl Cancer Inst* 1975;55:555–60.
 42. Tom BH, Rutsky LP, Jakstys MM, Oyasu R, Kaye CI, Kahan BD. Human colonic adenocarcinoma cells. I. Establishment and description of a new line. *In Vitro* 1976;12:180–90.
 43. Leibovitz A, Stinson JC, McCombs WB III, McCoy CE, Mazur KC, Mabry ND. Classification of human colorectal adenocarcinoma cell lines. *Cancer Res* 1976;36:4562–9.
 44. Boyd D, Florent G, Kim P, Brattain M. Determination of the levels of urokinase and its receptor in human colon carcinoma cell lines. *Cancer Res* 1988;48:3112–6.
 45. Aden DP, Fogel A, Plotkin S, Damjanov I, Knowles BB. Controlled synthesis of HBsAg in a differentiated human liver carcinoma-derived cell line. *Nature* 1979;282:615–6.
 46. Sugimoto T, Tatsumi E, Kemshead JT, Helson L, Green AA, Minowada J. Determination of cell surface membrane antigens common to both human neuroblastoma and leukemia-lymphoma cell lines by a panel of 38 monoclonal antibodies. *J Natl Cancer Inst* 1984;73:51–7.
 47. Soule HD, Vazquez J, Long A, Albert S, Brennan M. A human cell line from a pleural effusion derived from a breast carcinoma. *J Natl Cancer Inst* 1973;51:1409–16.
 48. Wascher RA, Huynh KT, Giuliano AE, et al. Stanniocalcin-1: a novel molecular blood and bone marrow marker for human breast cancer. *Clin Cancer Res* 2003;9:1427–35.
 49. Crnogorac-Jurcevic T, Efthimiou E, Nielsen T, et al. Expression profiling of microdissected pancreatic adenocarcinomas. *Oncogene* 2002;21:4587–94.
 50. Huang Y, Prasad M, Lemon WJ, et al. Gene expression in papillary thyroid carcinoma reveals highly consistent profiles. *Proc Natl Acad Sci U S A* 2001;98:15044–9.
 51. Kallakury BVS, Karikehalli S, Haholu A, Sheehan CE, Azumi N, Ross JS. Increased expression of matrix metalloproteinases 2 and 9 and tissue inhibitors of metalloproteinases 1 and 2 correlate with poor prognostic variables in renal cell carcinoma. *Clin Cancer Res* 2001;7:3113–9.
 52. Ruf W, Seftor EA, Petrovan RJ, et al. Differential role of tissue factor pathway inhibitors 1 and 2 in melanoma vasculogenic mimicry. *Cancer Res* 2003;63:5381–9.
 53. Kim K-A, Song J-S, Jee JG, et al. Structure of human PRL-3, the phosphatase associated with cancer metastasis. *FEBS Lett* 2004;565:181–7.

Molecular Cancer Therapeutics

Protein tyrosine phosphatase PRL-3 in malignant cells and endothelial cells: expression and function

Cecile Rouleau, Andre Roy, Thia St. Martin, et al.

Mol Cancer Ther 2006;5:219-229.

Updated version Access the most recent version of this article at:
<http://mct.aacrjournals.org/content/5/2/219>

Cited articles This article cites 51 articles, 15 of which you can access for free at:
<http://mct.aacrjournals.org/content/5/2/219.full#ref-list-1>

Citing articles This article has been cited by 9 HighWire-hosted articles. Access the articles at:
<http://mct.aacrjournals.org/content/5/2/219.full#related-urls>

E-mail alerts [Sign up to receive free email-alerts](#) related to this article or journal.

Reprints and Subscriptions To order reprints of this article or to subscribe to the journal, contact the AACR Publications Department at pubs@aacr.org.

Permissions To request permission to re-use all or part of this article, use this link
<http://mct.aacrjournals.org/content/5/2/219>.
Click on "Request Permissions" which will take you to the Copyright Clearance Center's (CCC) Rightslink site.